Low-Cost sensors for measuring wadi discharge - a Raspberry Pi based seismometer and time-lapse camera setup

Robert Krüger[1], Xabier Blanch[2], Jens Grundmann[3], Ghazi Al-Rawas[4], Anette Eltner[1]

[1] Institute of Photogrammetry and Remote Sensing, Dresden University of Technology, Germany
(robert.krueger; anette.eltner)@tu-dresden.de
[2] Department of Civil and Environmental Engineering, Universitat Politècnica de Catalunya, Spain – xabier.blanch@upc.edu
[3] Chair of Hydrology, Dresden University of Technology, Germany – jens.grundmann@tu-dresden.de
[4] Department of Civil and Architechtural Engineering, Sultan Qaboos University, Muscat, Oman – ghazi@squ.edu.om

Keywords: low-cost sensors, photogrammetry, environmental seismology, hydrology

Abstract

This study presents a low-cost, multi-sensor monitoring setup for wadi discharge assessment. The system comprises a time-lapse camera gauge and a Raspberry Shake seismograph, both powered by solar energy and integrated with data transmission units for remote monitoring. Optical data, combined with a high-resolution digital terrain model generated via UAV-based photogrammetry, enables semi-automatic discharge estimation. Seismic data complement the optical workflow by capturing flow-induced vibrations, providing a second line of evidence for wadi discharge. Our systems operated successfully, recording several flow events, highlighting the feasibility of low-cost, remote monitoring in ephemeral wadi environments. Key challenges included limited camera accuracy and the need for frequent DTM updates due to morphological changes. Improvements, such as upgrading camera hardware and enhancing automation in data processing, are underway to increase system accuracy and reliability for operational use.

1. INTRODUCTION

In recent years, Oman has experienced a rise in the frequency of flash floods (Abushandi and Al Ajmi, 2022). This trend is closely tied to climate change, which leads to an intensification of the atmospheric water cycle. The rapid expansion of urban areas, extending directly into wadis, combined with consequential increased soil sealing and inadequate drainage systems, further heightens the likelihood of flooding. This situation leads to substantial property damage and recurring loss of life. Despite the escalating threat posed by flash floods, Oman currently lacks early warning systems for accurate prediction and assessment of these events. Developing such a system requires densely distributed sensor networks to measure rainfall and wadi discharge. In addition to monitoring floods, recording runoff is essential for water management. However, due to the country's challenging topography and vast size, implementing these dense networks is not practicable, amongst other because of high cost.

Current local wadi observation networks consist of pressure or radar gauges. Both types have disadvantages. With the former, the installation in water entails the risk of losing the gauge in the event of flooding. The latter are often installed close to the edge of the ever-changing wadi channels – which often limits the measuring range towards medium and high flow scenarios. A solution to these challenges can be the application of image-based methods as cameras can be installed outside the channel while still being able to cover the whole river cross section. Several studies showed the potential to accurately measure water level with cameras, even applied in low-cost setups (Eltner et al., 2018). An additional benefit of using cameras is the potential to measure flow velocities, by capturing and processing short video sequences (Eltner et al., 2020, Grundmann et al., 2024), and eventually estimating discharge. However, the use of image-based methods has the disadvantage that their use is limited in difficult lighting conditions, especially at night given the usually large width of the wadi reaches.

Recently, seismic observations were utilized to infer river level and bedload flux (Dietze et al., 2019). These studies employed two physical models, which predict the seismic frequency spectra created by bedload transport (Tsai et al., 2012) and turbulent flow (Gimbert et al., 2014). Both models rely on a large number of parameters to be set, including water level. Therefore, Monte Carlo approaches are used to randomly sample parameters for synthetic spectra calculation to be compared against the empirical one (Dietze et al., 2019). Thereby, the best fitting solution is used to determine the bedload flux and water level.

A combination of cameras and seismic sensors can allow for a more robust and synergetic measurement of wadi discharge. Optical measurements of water level and surface velocities can better constrain model parameters used in the inversion of the seismic signals. This would provide a higher accuracy of water level estimation from the seismic signal in conditions, where image-based methods are not available, e.g., at night.

With low-cost seismometers now widely available, we propose a combined low-cost seismo-optical setup. This setup was installed at two reaches of Wadi Al-Hawasinah, Oman. We describe our low-cost setup in detail and we explain the general workflow for measuring water levels and discharge. Furthermore, we assess initial results from observed flow events and discuss the applicability of the chosen setup.

2. METHODS

2.1 Study area

The study area is the catchment of Wadi Al-Hawasinah in Oman's Al Batinah North governorate, a region significantly

impacted by cyclone Shaheen in October 2021. Covering 980 km², the catchment is fed by run-off from the Hajar Mountains and drains north-eastward into the Sea of Oman. Like most wadis in Oman, Wadi Al-Hawasinah has an ephemeral water flow, remaining dry for most of the year except during periods of rainfall. Wadi Al-Hawasinah is divided into two main sub-catchments, Hawasinah Southeast and Hawasinah Southwest, each monitored by reference gauges at their respective outlets.

We selected Ghuzayn (N23.818°, E56.986°) and Lihban (N23.803°, E56.892°), the outlet locations, as our study sites to provide reference measurements for our seismo-optical approach. At both sites, the channel is approximately 60 to 90 meters wide. Water levels are measured using radar sensors (SEBAPuls, Germany) mounted close to the outer bank and capturing data every 5 minutes (Figure 1) .

Figure 1. Radar gauging station in Lihban - during low flow conditions

In Ghuzayn, we installed our setup at the location of a former pressure gauge, which was destroyed during the Shaheen cyclone event. The station is positioned on the same side of the channel, approximately 330 meters upstream of a newly installed radar gauge (figure 2). In Lihban, our setup was installed at the same site of a previous pressure gauge, which has since been replaced by a new radar gauge (figure 3). Both systems were set up during the winter months of 2023/2024.

Both locations witnessed numerous flow events in February, March, and April 2024, with the most significant events occurring around April 16.

2.2 Acquisition of reference data

To produce a high-resolution terrain model (DTM), we used the Structure-from-Motion with Multi-View Stereo (SfM-MVS) algorithm, employing images captured by UAV. This method enables frequent model updates of the riverbed following changes due to high-flow events. For data acquisition, we used a DJI M210 UAV equipped with a MicaSense Altum camera, featuring 5 spectral bands (RGB, Red Edge, and NIR) at 3 megapixels each and an 8 mm fixed focal length.

The flights were conducted at an altitude of 110 meters, in 6–7 flight lines along the wadi channel, covering an area of approximately 8 hectares in Lihban and 13 hectares in Ghuzayn. The images were processed in Agisoft Metashape 2.0.1 to generate point clouds, DTMs (9.5 cm/px resolution), and orthophotos (ground resolution 4.8 cm/px). As flow was minimal in Ghuzayn and nonexistent in Lihban during the flights, nearly the whole channel was reconstructed.

To later convert image measurements into 3D space, both the camera and the DTM need to be referenced in the same coordinate system. For this purpose, permanent ground control points (GCPs) were established — 23 each in Ghuzayn and Lihban, measured with RTK GNSS to achieve 2 cm accuracy. Ten GCPs were positioned within the field of view of the respective camera system, with the remaining targets distributed across the UAV flight areas. All but two GCPs were used in the SfM-MVS workflow to accurately georeference the models, as the UAV did not have a high-precision GNSS system. For these, accuracies of 3.2 cm (Ghuzayn) and 4.4 cm (Lihban) could be established.

The interior camera parameters, of the fixed cameras to monitor the wadi channel were estimated via self-calibration using a temporary calibration field and using Metashape to derive focal length, principle point and distortion parameters.

2.3 Camera data processing

For the optical workflow a low-cost camera captures images and short video sequences. To determine the water level, convolutional neural networks (CNNs) are employed to segment the water area in the images. Next, the waterline, i.e. the border between water and shore, is identified and projected into object space, to be intersected with a high-resolution digital terrain model (DTM) as outlined by (Eltner et al., 2021) eventually leading to water level information for nearly each waterline pixel. Both, camera and DTM are georeferenced using GCPs placed in and around the area of interest. This allows for localization and orientation of the camera via spatial resection and subsequently projecting the segmented water area from the images into the DTM, all observations being now available in the same coordinate system.

To estimate time series of discharge, the OptiQ modeling approach is employed (Grundmann et al., 2024). The method utilizes surface flow velocities and channel properties as input parameters. Surface flow velocities are measured in image sequences by tracking particle using the AI-based Pips++ technique (Harley et al., 2022). The resulting particle tracks are then projected into object space and intersected with the water surface assumed as a plane at the water level height. The wetted river cross-section is extracted from the same high-resolution DTM used for the water level estimation. Finally, the surface velocities are depth-averaged and multiplied by the cross-section area to get the discharge.

2.4 Seismic data processing

For this study, seismic signals were interpreted solely visually. Thus, spectrograms, a visual representation of the spectrum of frequencies of a seismic signal, were computed. To assess its relationship to wadi flow events, it was overlayed with discharge data from the reference gauges. The seismic data was processed with the Python library "ObSpy" and the R package "eseis" (Dietze, 2018). The former was used to remove the instrument response of the Raspberry Shake geophone from the seismic signal. The required response metadata can be downloaded from the Raspberry Shake website. The R package "Eseis" was used to compute the spectrogram using the Welch method with 30 s long windows overlapping by 80 %. The inversion method mentioned in the introduction is beyond the scope of this study.

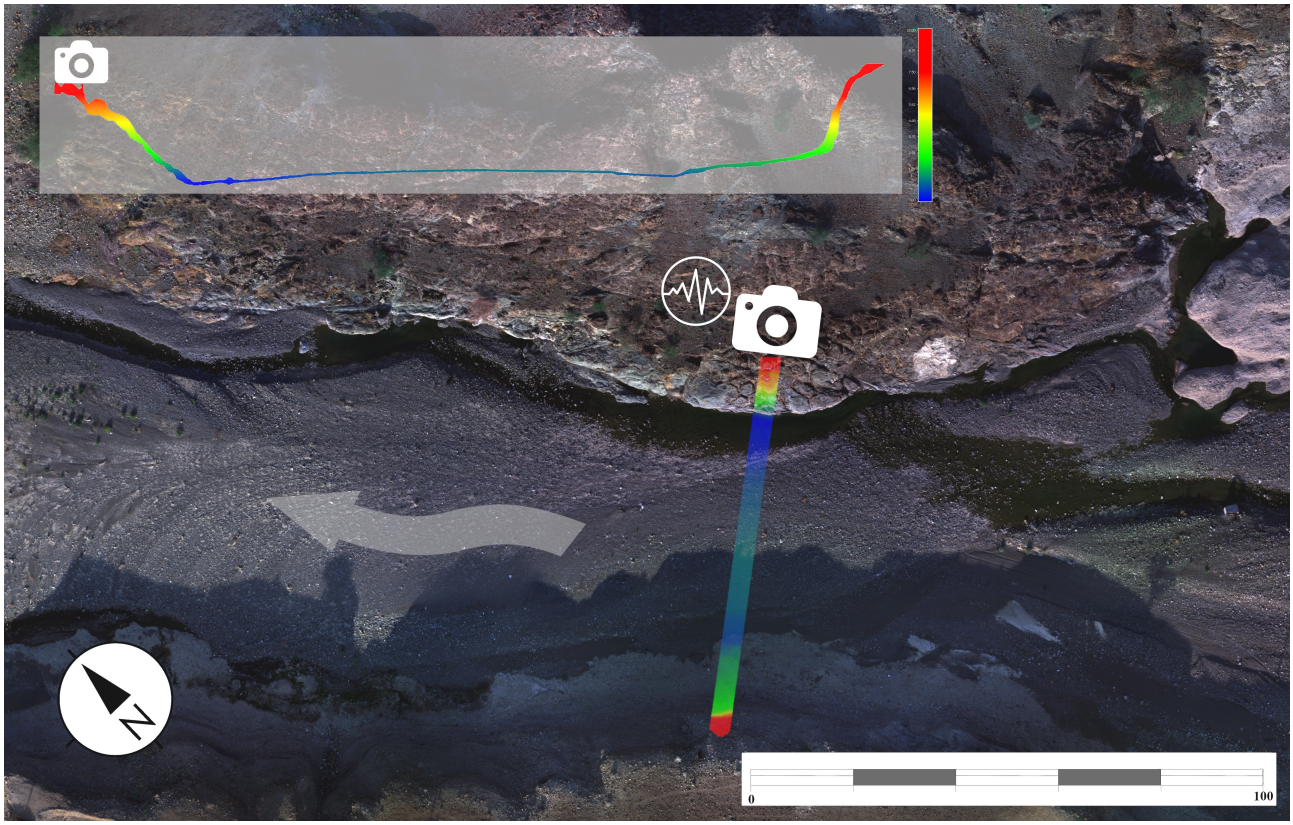

Figure 2. UAV based orthophoto of the study area in Ghuzayn. Locations of camera- and seismic-system are shown in the map. Further, the cross-section of interest is indicated in red-yellow-green-blue colours and as profile in the top left corner. The height of the cross-section ranges from 0 m (blue) to 10 m (red).

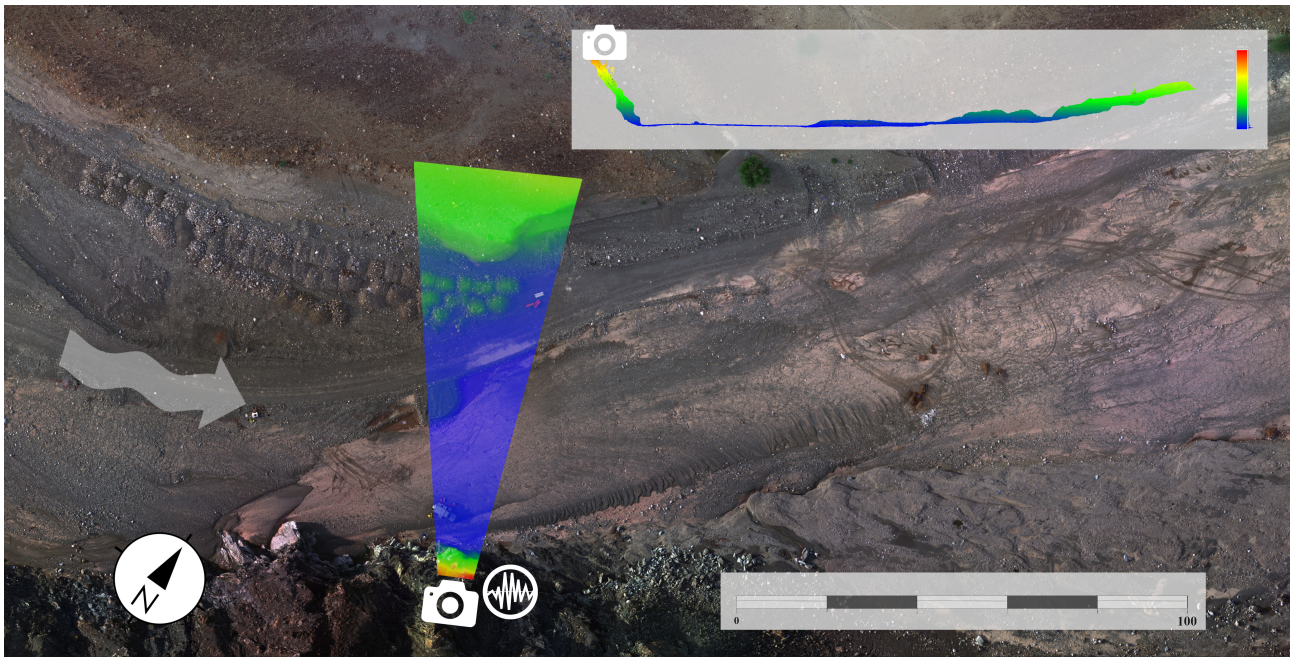

Figure 3. UAV based orthophoto of the study area in Lihban. Locations of camera- and seismic-system are shown in the map. Further, the cross-section of interest is indicated in red-yellow-green-blue colours and as profile in the top right corner. The height of the cross-section ranges from 0 m (blue) to 18 m (red).

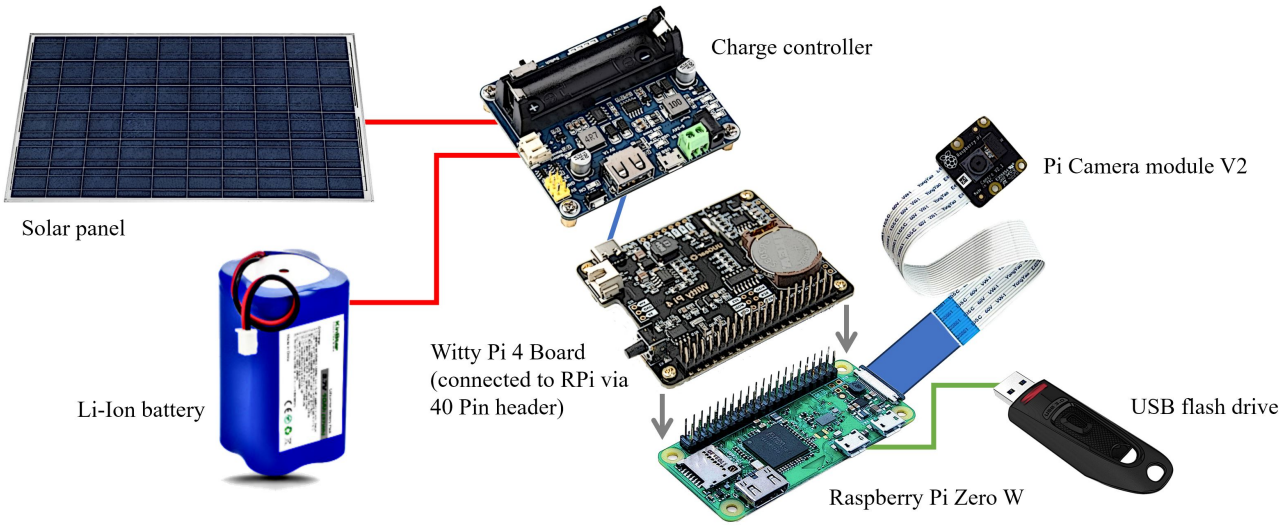

Figure 4. schematic illustration of the camera system. Raspberry Pi and WittyPi Board are connected through the 40 Pin GPIO Header. Charge controller is screwed on top of the Raspberry Pi assembly. Power for the WittyPi is provided via a short USB-Cable. The camera is connected to the Pi via a flat ribbon cable and the respective Port on the board. USB Flash Drive is connected via Micro-USB adapter.

3. LOW-COST SETUP

The presented setup comprises two measurement devices: a time-lapse camera system and a low-cost seismograph, both of which can function independently. Additionally, these devices have been combined with a data transmission unit, transforming them from simple data acquisition tools into real-time monitoring systems. The whole setup is controlled by a Raspberry Pi single board computer (SBC). The following section provides a detailed description of these systems, emphasizing the hardware and software components used to enhance the reproducibility of the proposed setup.

3.1 Low-cost time-lapse camera gauge

3.1.1 Hardware: The setup is based on earlier studies for detection of rockfalls (Blanch et al., 2023, Blanch et al., 2024) and river stage monitoring (Eltner et al., 2018). These studies showed that a low-cost system designed around a widely available SBC - the Raspberry Pi, can be utilized for environmental monitoring. In this study, we used the Raspberry Pi camera V2 module. For this sensor, temperature related instability of the inner orientation parameters is a known problem (Elias et al., 2020), which affects measurement accuracy especially in desert climates with high temperature fluctuations. However, due to limited availability of the V3 module, we had to rely on this older camera.

To operate the camera, manage data storage, and handle the transmission of captured images and videos, integration with a Raspberry Pi system is needed. The proposed system prioritizes energy efficiency to enable prolonged operation without frequent battery replacements and facilitating recharging via solar panels. Powering any Raspberry Pi with solar panels is relatively straightforward in a region like Oman. The Raspberry Pi Zero W was selected for its minimal energy consumption and the lowest acquisition cost within the Raspberry Pi product lineup. If an application requires on-board data processing, a more powerful (and correspondingly more energy-intensive) model might be needed.

To measure wadi discharge, the system needs to capture images and videos at frequent intervals. In this study, we selected a 15-minute interval, allowing the system to shut down completely between camera operations to conserve energy. Since the Raspberry Pi does not have an internal battery, its real-time clock (RTC) is disabled when the system powers down. To address this limitation, we incorporated an external RTC. Specifically, we used the UUGear WittyPi 4 Board, which not only adds RTC functionality but also enhances power management, enabling scheduled wake and sleep cycles for the Pi.

The camera system is powered by a Lithium battery (3.7 V, 1S4P configuration / 48 Wh), which is charged via an attached solar panel of approximately 40 Wp. To manage the energy flow, we employ a Waveshare solar charge controller. This device not only regulates the charging process but also features an internal step-up converter that provides a 5V output, making it convenient to power the Raspberry Pi system directly. A schem

All components, except for the solar panel, are housed in a waterproof and dustproof enclosure. Inside, the Raspberry Pi is mounted on a 3D-printed baseplate, which is securely glued to the bottom of the enclosure. The WittyPi board is attached to the top of the Raspberry Pi using the 40-pin header and supported by additional screws, as its size exceeds that of the Raspberry Pi. The charge controller is fixed on top of the WittyPi board using screws, and it powers the WittyPi through a USB cable. The enclosure also includes the battery, which connects to the charge controller, and a USB drive connected to the Raspberry Pi . The camera is mounted at the top of the enclosure using a small mounting plate, with a laboratory glass window glued in place to protect the opening for the camera. The cable to the solar panel is routed outside through a sealed cable gland. The enclosure can be mounted to a pole using a ball head attached to its rear side.

A schematic illustration of the whole system can be seen in figure 4, while figure 5 shows the assembled system.

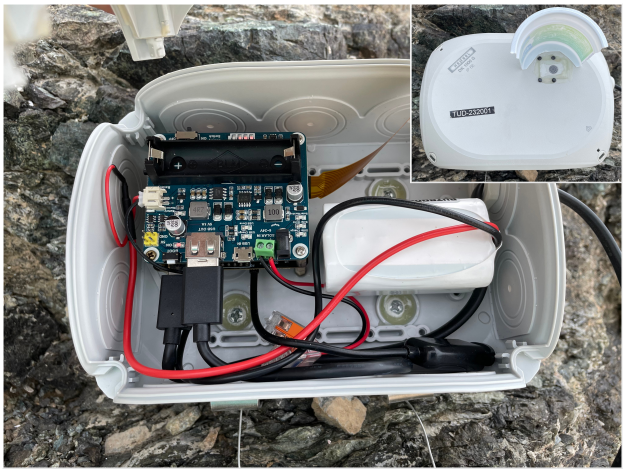

Figure 5. Camera system in waterproof containment. Stack of modules (Raspberry Pi, WittyPi and charge-controller on top) on the left, with USB flash-drive (bottom), battery (white) and camera connected with ribbon cable. Top right image depicts lid of containment with camera opening.

3.1.2 Software: This section outlines the software for capturing images and video sequences, as well as the basic requirements for running our system.

In our setup, we utilized Raspberry Pi OS (operating system) Lite, which does not include a desktop environment, as our systems will operate headlessly at all times.

The required and installed WittyPi software manages the RTC of the Pi, either using the internal clock of the WittyPi or syncing with internet time (when available) to prevent RTC drift. It further handles executing additional scripts, as well as system shutdown and wake-up according to a custom schedule. In our case, the schedule is set between 5 a.m. and 8 p.m., during which the system powers on every 15 minutes, runs for 3 minutes to complete its tasks, and then shuts down.

The software to capture the image data is implemented in Python and follows a sequence of operations. The run of the corresponding source code is started by the WittyPi software. The following steps are organized within the script:

1. Mount the USB Flash Drive: To enable data storage and retrieval.
2. Check Daylight Conditions: To check whether the current time falls within the window from 30 minutes before sunrise to 30 minutes after sunset. If this condition is met (indicating daylight), the workflow proceeds.
3. Capture and Save an Image: To acquire and save the image to the mounted flash drive.
4. Capture and Save a Video Sequence: A 7-second video sequence is recorded and saved to the mounted flash drive.
5. Save Log Files: Log files documenting the success of the software operation for record-keeping and debugging purposes. The logfiles created by the WittyPi software are copied to the same folder
6. Send single Image via Email: If the current time matches a specific trigger (here: 4 p.m.), the latest captured image is sent via email for monitoring purposes.
7. *Upload of Data to Cloud Service: A direct upload of the captured images and videos to cloud services as Google Drive or Dropbox is possible, although not used in our project.*

The Python code and additional installation details are available in the author's repository (github.com/kruegertud/WadiLowCost).

3.2 Raspberry Shake seismograph

The Raspberry Shake is a low-cost, all-in-one seismic sensor and extension board designed for the Raspberry Pi. For this project, we used the RS1D model, which features a vertical-component 4.5-Hz geophone paired with a 24-bit internal digitizer capable of recording data at 100 Hz resolution (Anthony et al., 2019). The installation process is simple: the geophone connects to the digitizer board using a screw terminal, and the board is then attached to the Raspberry Pi's 40-pin connector (figure 6). The software setup is equally straightforward, as the system comes with a pre-configured Raspberry Pi OS available for download from the manufacturer's website. This OS only needs to be written to an SD card to complete the setup. Note, that another Raspberry Pi is used to control the seismograph.

To maintain accurate timing for the seismic measurements, the Raspberry Shake relies on either an internet connection for network time protocol (NTP) synchronization or a connected GNSS antenna. Although our system was designed for continuous internet connectivity, we added a Roblox GNSS chipset and antenna as a backup, connected via a USB-serial adapter. This GNSS board also provides a Pulse Per Second (PPS) signal for enhanced timing synchronization, which we connected to Pin 40 of the Raspberry Pi.

Data upload can be configured for real-time transmission directly to the Raspberry Shake servers, which is managed automatically through the Shake OS. To conserve bandwidth and reduce transmission costs, we decided to upload the stored data (mseed files) to a cloud service once daily, instead, to reduce data sent from 71-121 MB (Raspberry Shake S.A., 2021) to approximately 10 MB per day. This process was automated using a Python script scheduled with the cron job service.

Similar to the camera system, the Raspberry Shake needed to be housed in a dust- and waterproof enclosure. Ensuring a firm connection between the geophone and the enclosure was crucial for precise measurements. To achieve this, we utilized a 3D-printed baseplate that secured both the Raspberry Pi and the geophone, which was then glued to the enclosure. The printing files for the baseplate and clamps holding the geophone were sourced from the Raspberry Shake website. Cables for GPS-antenna, power supply and network connection are routed outside through sealed cable glands. A bubble level was mounted on the lid of the enclosure to ensure horizontal alignment during installation (see figure 7).

Unlike the camera systems, which operate for only 12 minutes per hour during daylight, the seismic system runs continuously. Additionally, the Raspberry Pi 3B+ used in this setup has significantly higher power consumption, drawing 2.8 watts during startup and 1.5 watts during standard operation (Raspberry Shake S.A., 2021). To support this energy requirement, the system is powered by a 50 WP solar panel connected to a 12V lead-acid car battery. Since the Raspberry Pi requires a 5V input voltage, we incorporated an isolated DC/DC converter (Traco

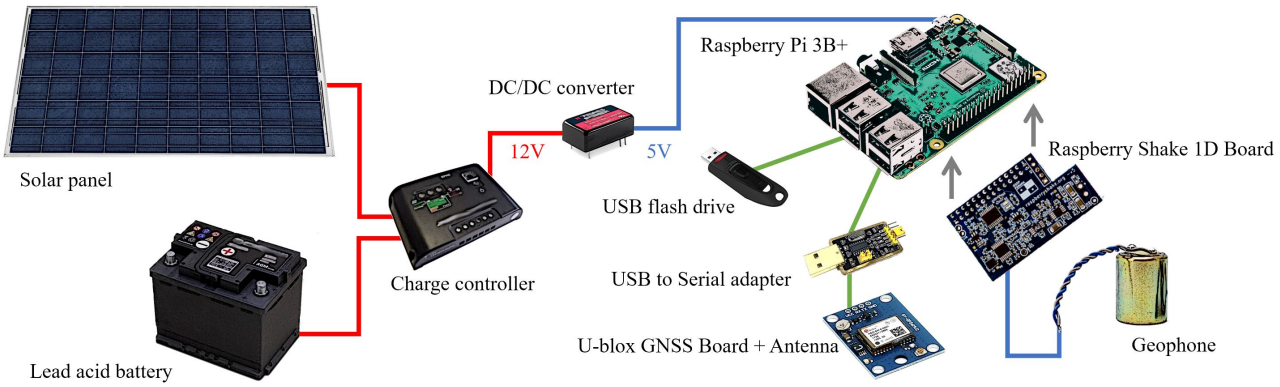

Figure 6. Schematic illustration of the seismic system. Raspberry Shake board is connected to the Raspberry Pi on the 40 Pin GPIO Header. Flash-drive and GNSS are connected through the RPi's USB Ports.

Figure 7. Raspberry Shake system mounted in waterproof enclosure, with GNSS antenna connected (left) and bubble level mounted to the lid (right).

Tel 10-1211) to step down the voltage. The use of an isolated DC/DC converter helps prevent electrical interference from affecting the seismic signals, ensuring integrity of the data.

The system was installed by positioning the enclosure on exposed bedrock near the camera gauge, covering it with a layer of stones and rocks. This shielded the system from direct exposure to rain and wind.

3.3 Data transmission

For data transmission, we utilized an USB-powered 4G modem with an integrated WiFi access point. The data transmission unit was placed in the external box of the seismic system and powered through the same battery solar panel combination.

Both sensing systems, i.a. the Pi controlling the camera and the Pi controlling the Shake, connected to this access point — either using built-in WiFi for the former or an external WiFi dongle for the latter.

To facilitate remote access for monitoring, maintenance, and data retrieval, we employed the ZeroTier service. ZeroTier is a web service that creates private virtual networks, enabling secure connections between devices regardless of their physical locations. To implement this, a client application must be installed on each system connecting it to the private virtual network. Within this network, every device is assigned a static IP address, which remains constant even if their respective IP on the 4G network changes. This feature allows users to seamlessly connect to the systems via SSH or SFTP or access the Raspberry Shake's configuration web-interface.

To facilitate remote access for the camera systems, we scheduled a 30-minute maintenance window (e.g., 1200–1230 UTC) utilizing the WittyPi's scheduling feature. During this time, the systems remained active and operational, preventing any shutdowns.

4. RESULTS AND DISCUSSION

4.1 Low-cost time-lapse camera gauge

Both camera systems have been operating continuously since their installation, capturing images and videos at 15-minute intervals. Daily image updates, sent via email, were utilized to monitor and detect flow events. For Ghuzayn, 11 flash floods of different sizes have been recorded between February 12th and October 16th. However, many peak flow episodes went undocumented because they occurred during nighttime, including the largest flash flood events on April 16th and 17th, 2024.

The semi-automatic workflow for water level detection was tested on smaller flow events, e.g., the 29-02-24 event (Figure 8). However, achieving high accuracy in water level measurements requires careful consideration of several potential sources of error:

GCPs: While the real-world positions of GCPs were measured with high accuracy, their identification in the images presented challenges. The markers used (sprayed crosses), combined with the distance from the camera (70–90 meters to the GCPs at the opposite riverbank), made it difficult to pinpoint their exact location in the images with sub-pixel precision. Additionally, the

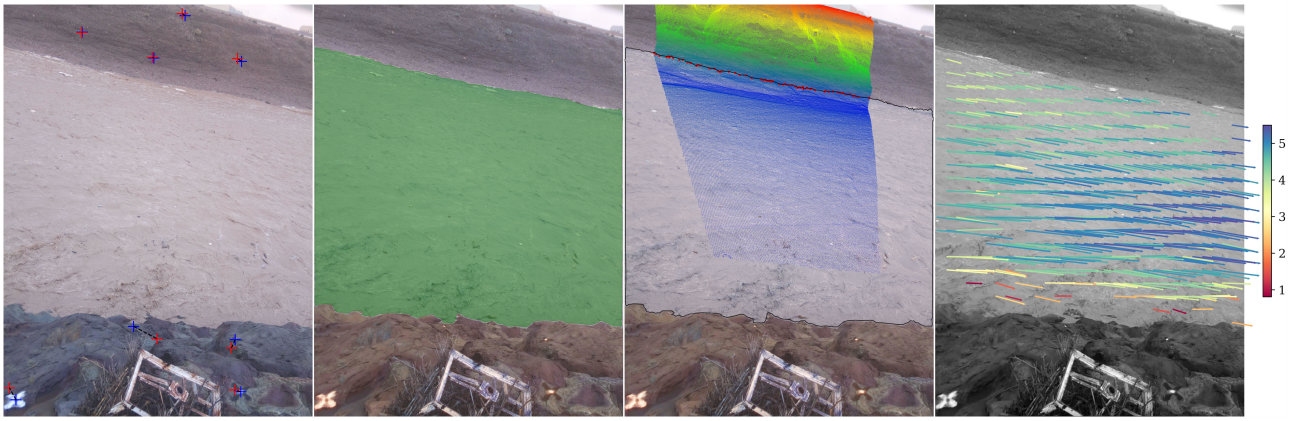

Figure 8. Data processing steps of the optical workflow for the event on 29-02-24 15:15 in Ghuzayn (from left to right): a) GCP measured in image (blue) and RTK-GNSS measured GCP projected into image (red), b) AI-based segmented water area (green), c) polygon border of segmented water (i.e. waterline) intersected with DTM (nearest points from DTM marked as red dots, DTM height marked in blue to red) to obtain water-level (1.94 m, std = 0.30 m), d) measured particle tracks (using Pips++) in video sequence (which were projected into object space to be intersected with water surface to estimate surface velocities in [m/s])

spatial distribution of the GCPs is suboptimal, as they form two lines along the riverbanks at similar heights, i.e. the points lie roughly within a plan. Since placing GCPs within the riverbed is not feasible, no alternative solution is available.

Camera quality/stability: In addition to the quality of the GCP markers, the imaging quality of the camera emerged as a significant source of error. Areas of the images were often blurry, making it challenging to accurately measure the GCP positions within them. Although the camera's interior parameters were estimated during self-calibration, the spatial resection error was notably high (66.3 pixels) for the dataset shown in Figure 8. This is due to a combination of the factors mentioned earlier, with the overall quality of the low-cost sensors, such as the cheap plastic lens, limited sensor size with a very low pixel pitch, and temperature-related instability (Elias et al., 2020). This has a strong impact on the reliable estimation of the external geometry of the camera, especially considering the latter point because the interior camera parameters were kept fixed during the spatial resection while a temporal stability cannot be assumed.

Water segmentation: While the applied CNN-based segmentation methods are effective (Eltner et al., 2021), the large distance of the observed river bank can amplify the impact of small measurement errors, necessitating careful consideration in the interpretation of water level data.

DTM: The quality of the Digital Terrain Model (DTM) is essential for accurate water level estimation, as image measurements are intersected with the DTM to derive these estimates. In our study, the DTM had a resolution of 9.5 cm, which imposes a corresponding limit on the achievable precision. However, errors in the estimation of the internal and external geometry had a more significant impact on our results, which can be emphasised by the fact that the obtained water level values along shore line are fluctuating strongly - as the obtained line and the DTM are not aligned well. Furthermore, during the observation period, we noted substantial visual changes in the riverbed, underscoring the necessity for frequent updates of the 3D model — particularly after significant flow events. This can be accomplished through either a new UAV survey or by employing a second camera to leverage stereo-photogrammetry.

4.2 Raspberry Shake seismograph

Multiple flow events were captured by the seismic sensors since installation. A typical spectrogram for flash flood events can be seen in Figure 9. A strong rise in seismic energy from 10 Hz to 50 Hz is visible with the onset of the flood at 18.30 UTC (22.30 local time). Further it becomes obvious that most seismic energy is recorded at about 30 Hz, other peaks are at 16 Hz, 23 Hz and another cluster at 35-50 Hz. Discharge peaked at 18.40 UTC (22.40 local time), subsequently the water level fell again, so did seismic energy. In the later stage, there were some seismic bands still active (12 Hz) which might relate to turbulent flow in the wadi channel (Dietze et al., 2019).

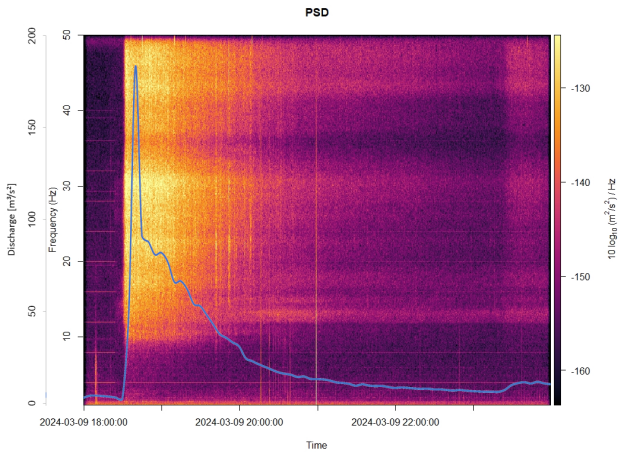

Figure 9. Flashflood event in Lihban 09-03-2024. Spectrogram overlayed with discharge from reference gauge (in blue) [m³/s]

4.3 General observations and outlook

From a technical perspective, the systems have demonstrated that a low-cost sensor solution for wadi discharge is feasible. By leveraging favourable solar conditions, we were able to implement a remote installation, with no battery-related failures observed. However, connectivity issues have occurred at both locations, resulting in intermittent loss of connection, which could only be resolved by restarting the 4G modem. This issue necessitated technician visits to the site, incurring both time

and financial costs. Switching to a different modem type would likely enhance system reliability and reduce the need for such interventions.

Sensor-wise both types have shown, that they are able to capture flow events of different size. The Pi Camera V2 allows for measurements of only limited quality and will therefore be swapped to the V3 model with a higher sensor resolution and size to potentially increase the accuracies.

Another key task will be the regular update of the DTM of the wadi channel. This is crucial for both the camera-based workflow and seismic inversion applications. For instance, estimating parameters such as grain size distribution and bed roughness requires high-resolution DTMs and/or imagery. Further UAV surveys will be conducted and a stereo system will be installed at each site.

5. CONCLUSIONS

The implementation of a low-cost monitoring system in Wadi Al-Hawasinah demonstrates the feasibility of using accessible technologies for wadi discharge assessment in remote arid regions. Both the time-lapse camera gauge and the Raspberry Shake seismograph successfully captured flow events, providing complementary data for understanding wadi hydrodynamics. Despite challenges related to camera quality, data transmission reliability, and the dynamic nature of wadi morphology, the system proved robust under harsh environmental conditions. Future developments include upgrading to higher-quality cameras, automating key aspects of the optical workflow, and regular updates to the DTM to account for morphological changes. These improvements aim to enhance measurement accuracy and reduce manual intervention, paving the way for operationalizing this low-cost approach in similar environments. This study underscores the potential of integrating low-cost optical and seismic sensors for comprehensive wadi monitoring and highlights the importance of interdisciplinary methods in addressing hydrological challenges in ephemeral river systems.

ACKNOWLEDGEMENTS

We express our gratitude to Dr. Malik Al-Wardy for conducting the field survey. We also sincerely thank Halwalage Induka Nilupul for his invaluable support in maintaining the performance of our sensor systems. Additionally, we deeply appreciate Dr. Michael Dietze for his insightful guidance on the topic of environmental seismology. Finally, we thank Leonardo Bruno for the initial tracking tests with Pips++.

References

Raspberry Shake S.A., 2021. Raspberry shake technical specifications. https://manual.raspberryshake.org/downloads/ RS-GlobalTechnicalSpecificationsDocument.pdf, 2024-11-03.

Abushandi, E., Al Ajmi, M., 2022. Assessment of Hydrological Extremes for Arid Catchments: A Case Study in Wadi Al Jizzi, North-West Oman. *Sustainability*, 14(21). doi.org/10.3390/su142114028.

Anthony, R. E., Ringler, A. T., Wilson, D. C., Wolin, E., 2019. Do Low-Cost Seismographs Perform Well Enough for Your Network? An Overview of Laboratory Tests and Field Observations of the OSOP Raspberry Shake 4D. *Seismological Research Letters*, 90(1), 219–228. doi.org/10.1785/0220180251.

Blanch, X., Guinau, M., Eltner, A., Abellan, A., 2023. Fixed photogrammetric systems for natural hazard monitoring with high spatio-temporal resolution. *Natural Hazards and Earth System Sciences*, 23(10), 3285–3303. doi.org/10.5194/nhess-23-3285-2023.

Blanch, X., Guinau, M., Eltner, A., Abellan, A., 2024. A cost-effective image-based system for 3D geomorphic monitoring: An application to rockfalls. *Geomorphology*, 449, 109065. doi.org/10.1016/j.geomorph.2024.109065.

Dietze, M., 2018. The R package "eseis" – a software toolbox for environmental seismology. *Earth Surface Dynamics*, 6(3), 669–686. doi.org/10.5194/esurf-6-669-2018.

Dietze, M., Lagarde, S., Halfi, E., Laronne, J. B., Turowski, J. M., 2019. Joint Sensing of Bedload Flux and Water Depth by Seismic Data Inversion. *Water Resources Research*, 55(11), 9892–9904. doi.org/10.1029/2019WR026072.

Elias, M., Eltner, A., Liebold, F., Maas, H.-G., 2020. Assessing the Influence of Temperature Changes on the Geometric Stability of Smartphone- and Raspberry Pi Cameras. *Sensors*, 20(3). doi.org/10.3390/s20030643.

Eltner, A., Bressan, P. O., Akiyama, T., Gonçalves, W. N., Marcato Junior, J., 2021. Using Deep Learning for Automatic Water Stage Measurements. *Water Resources Research*, 57(3). doi.org/10.1029/2020WR027608.

Eltner, A., Elias, M., Sardemann, H., Spieler, D., 2018. Automatic Image-Based Water Stage Measurement for Long-Term Observations in Ungauged Catchments. *Water Resources Research*, 54(12), 10,362–10,371. doi.org/10.1029/2018WR023913.

Eltner, A., Sardemann, H., Grundmann, J., 2020. Technical Note: Flow velocity and discharge measurement in rivers using terrestrial and unmanned-aerial-vehicle imagery. *Hydrology and Earth System Sciences*, 24(3), 1429–1445. doi.org/10.5194/hess-24-1429-2020.

Gimbert, F., Tsai, V. C., Lamb, M. P., 2014. A physical model for seismic noise generation by turbulent flow in rivers. *Journal of Geophysical Research: Earth Surface*, 119(10), 2209–2238. doi.org/10.1002/2014JF003201.

Grundmann, J., Blanch, X., Kutscher, A., Hedel, R., Eltner, A., 2024. Towards a comprehensive optical workflow for monitoring and estimation of water levels and discharge in watercourses. *EGU General Assembly 2024*. doi.org/10.5194/egusphere-egu24-12507.

Harley, A. W., Fang, Z., Fragkiadaki, K., 2022. Particle Video Revisited: Tracking Through Occlusions Using Point Trajectories. arXiv:2204.04153 [cs].

Tsai, V. C., Minchew, B., Lamb, M. P., Ampuero, J., 2012. A physical model for seismic noise generation from sediment transport in rivers. *Geophysical Research Letters*, 39(2). doi.org/10.1029/2011GL050255.